COBEM 2023 27TH INTERNATIONAL CONGRESS OF MECHANICAL ENGINEERING

ABCM Brazilian Society of Mechanical Sciences and Engineering
27th ABCM International Congress of Mechanical Engineering
December 04-08, 2023, Florianópolis-SC, Brazil

COB-2023-0258
ANALYSIS OF THE INTERNAL CURVATURE OF AIR BENT PLATES AND ITS INFLUENCE ON PUNCH DISPLACEMENT

Pedro Henrique Marmilicz Kucarz
Milton Luiz Polli
Walter Luis Mikos
Federal University of Technology - Paraná, Av. Sete de Setembro, 3165 - Rebouças CEP 80230-901 - Curitiba - PR – Brasil
e-mails: pedro.kucarz@gmail.com, polli@utfpr.edu.br, e-mail: mikos@utfpr.edu.br

Paulo Victor Prestes Marcondes
Federal University of Paraná, Av. Cel. Francisco H. dos Santos, 230 - Centro Politécnico CEP 81530-000- Curitiba - PR - Brasil
e-mail: marcondes@ufpr.br

Abstract. *The internal curvature of sheets generated during air bending, using punch and die, has been simplified to the geometry of a semicircle. However, this simplification introduces errors in the calculations of punch penetration on the sheet and in the length of the raw material during sheet flattening. In this work, the verification of the curvature of the bent sheet was conducted by using test specimens bent in dies, and their profiles was measured. Results indicate that the curvature geometry is not similar to that of a semicircle, but rather resembles a parabola.*

Keywords: *Air bending, Inner radius, Punch displacement, Press Brake.*

1 INTRODUCTION

Bending forming, also known as folding or bending, is widely used due to its simplicity and efficiency as a manufacturing process. According to Benson (2015a), the bending process is present in a large number of forming industries, with air bending being the most common method. The process of air bending sheets offers great flexibility as it allows for bending at different angles and lengths using the same set of die and punch while achieving good measurement repeatability.

In 2020, the classification of machine tools for punching or chamfering, rolling, bending, and shearing, categorized under the PRODLIS code 2840.2170, which includes bending machines under the NCM code 8462.23.00, generated approximately R$1,143,230,000.00 in Brazil, with a volume of 9,583 units sold (IBGE, [*s. d.*]). This demonstrates the economic significance of this segment in the Brazilian market.

The air bending process in press brakes has greatly advanced with the implementation of CNC machines, which allow for precise positioning of the punch to achieve a specific bending angle. However, CNC-controlled press brakes do not provide this function, requiring operators to perform multiple empirical tests to achieve the desired angle in the workpiece. Analytical calculations for punch displacement on the sheet result in errors due to the simplification of the internal curvature geometry to a single radius. This simplification error leads to a phenomenon known as overbend, where the internal angle is insufficient, meaning the punch displaces less than it should (Ridane *et al.*, 2005). Another error caused by the simplification is in calculating the raw material geometry or cutting plan, resulting in errors in the length of the bent flanges.

Several equations simplify the internal curvature of the air-bent sheet; however, they do not provide the associated error for each equation. Furthermore, there is no consensus on whether the same simplification should be applied to both cases (punch displacement and raw material length). In this paper, it was verified which of the existing methods for calculating punch displacement, associated with the internal curvature formed during bending, provides results closest to practical measurements of punch displacement on the sheet for a given internal angle.

2 AIR BENDING

The bending process occurs in the plastic deformation regime. This regime is achieved due to an increase in stress on the sheet caused by the contact of the punch, resulting in the material exceeding its yield strength. At this point, the crystal lattice connections start to break, initiating the process of dislocation slip, which occurs along the densest planes of the unit cells. The movement of dislocations occurs from within the grains toward their boundaries and can be transferred to other grains if their families of crystallographic planes are aligned. Due to the movement of dislocations and the repositioning of unit cells, the sheet retains its deformed geometry even after the removal of the punch, thus completing the process of plastic deformation (Hertzberg *et al.*, 2012).

The operational simplicity of the bending process, coupled with the excellent stiffness-to-weight ratio of the bent parts, makes bending a competitive manufacturing process when compared to others. Air bending is the most commonly used method for sheet metal bending due to its speed, versatility, and simplicity. In this process, the punch penetrates into a sheet supported by the shoulders of the V-die, as shown in Figure 1. The final angle of the bend depends on the relative position between the punch and the die, where a deeper punch penetration results in a sharper internal angle of the bent part. Since the angle of the part depends solely on the punch displacement, it is possible to achieve bends with various angles using a universal set of tools on sheets of different thicknesses (Lange, 1985).

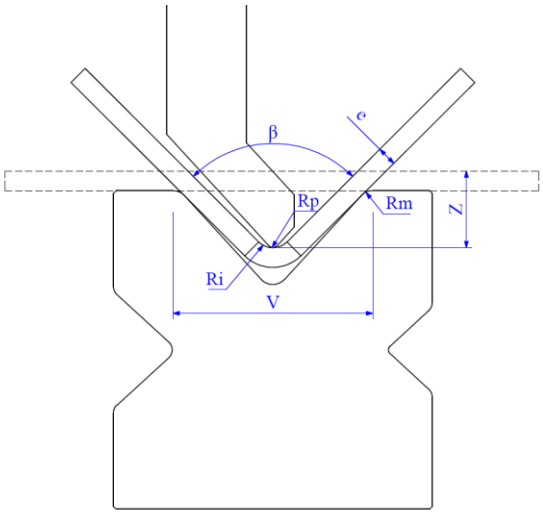

Figure 1. Main geometries of air bending, considering thickness e, die with opening V, displacement Z, internal angle β, internal radius R_i, radius at the tip of the punch R_p and radius on the shoulders of the die R_m.

2.1 Internal radius

Several authors have presented theories on the curvature geometry of air-bent sheet metal. Due to the transition region from elastic to plastic deformation, known as the elastoplastic region, analytical calculations become complex (De Vin *et al.*, 1994). Thus, a simplification to a purely plastic deformation geometry is adopted, and to achieve this, it is necessary to transform the curvature geometry into something known, with the geometry of a semicircle (radius) being the most accepted. One of the approaches used is the wrap-around effect, which assumes that the sheet metal immediately below the punch mimics the punch geometry. This approach is quite accurate when using punches with large radii at the tip, although it is not common due to the universality of dies and punches.

One of the more recent methods was presented by Benson, where he suggests that the internal curvature closely resembles that of a parabola. He also points out that, for punch displacement calculations, if we equate the perimeter of the parabolic curvature to that of a semicircle, the resulting radius is more accurate in existing analytical models (Benson, 2015b). Table 1 presents the known equations for simplifying the curvature geometry.

Table 1. Equations for calculating the internal radius with their respective origins.

Equation		Origin
$R_i = \frac{V}{6}$	(1)	Thumb rule
$R_i = 0{,}16 \cdot V$	(2)	Thumb rule
$R_i = R_p$	(3)	Wrap around
$R_i = \frac{V}{6{,}4}$	(4)	(Miranda *et al.*, 2014)
$R_i = 0{,}183 \cdot W - 3{,}43$	(5)	(Vin *et al.*, 2000)
$R_i = \frac{W \cdot tan\left(\frac{\beta_{krig}}{2}\right) + \frac{e}{2} - (Z - e)}{sec\left(\frac{\beta_{krig}}{2}\right) - 1}$	(6)	(Strano *et al.*, 2018)
$R_i = H_r - 2 \cdot (e^2)$	(7)	(Benson, 2015a)
$R_{ia} = H_{ra} - 2 \cdot (e^2)$	(8)	(Benson, 2015b)

2.2 Springback

The main phenomenon that occurs after removing the force applied by the punch on the sheet is springback. When the stress is released from the bent part, the regions that were elastically deformed return to their initial position. The primary effect of springback in air-bent parts is the difference in the internal angle after the load is removed. It is common for the internal angle to increase and become more obtuse after springback.

Since springback is caused by areas of elastic deformation, increasing the plastic deformation region of an air-bent part can reduce the elastic effect. To increase the plastic region, it is necessary to decrease the ratio of the die channel width to the sheet thickness (Miranda *et al.*, 2014).

The phenomenon of springback can be considered in the equations of punch displacement by using the Springback factor K_R. This factor causes the angle inserted in the equations to be sharper, resulting in the punch penetrating more than necessary, equation (10). However, after elastic rebound, the desired angle is achieved. The factor can be found in the Table 2.

$$K_R = \frac{\beta}{\beta_{Kr}} \tag{9}$$

Table 2 - Springback factor

Material	Springback factor K_R	
	$r_{i2}/_e = 1$	$r_{i2}/_e = 10$
St 0-24, St 1-24	0,99	0,97
St 2-24, St 12	0,99	0,97
St 3-24, St 13	0,985	0,97
Stainless austenitic steels	0,96	0,92
High temperature ferritic steels	0,99	0,97
High temperature austenitic steels	0,982	0,955
Nickel W	0,99	0,96
Al 99 5 F7	0,99	0,98
Al Mg 1 F 13	0,98	0,90
Al Mg Mn F 18	0,985	0,935
Al Cu Mg 2 F 43	0,91	0,65
Al Zn Mg Cu 1,5 F49	0,935	0,85

Source: Adapted from (Schuler, 1998)

Another method to estimate the springback effect is by comparing the ultimate stresses of different materials. This method is considered a rule of thumb, but it often yields good results for many cases (BENSON, 2015b). This method requires a known K_R, which can be determined through practical tests using equation (10). The equation for K_r for various materials is presented below.

$$K_r = 1 - \left[(1 - K_R) \cdot \frac{L_r}{L_c}\right] \tag{10}$$

2.3 Punch penetration calculation

Over the past three decades, researchers have been developing analytical equations to predict punch displacement and bending geometry. However, due to the complexity of the geometry during and after bending, analytical equations have been developed that only approximate the real penetration value. As a result, it is common for operators to make adjustments to the displacement during the first bend. After the initial adjustment, subsequent parts tend to come out consistently.

One of the simplest and most accurate methods was presented by De Vin where the bending deformation is considered purely plastic, treating the elastoplastic and elastic deformation regions as straight lines (rigid regions). The equation is derived from trigonometric relationships among the die, punch, and sheet. It considers the point where the angle β is reached as the final displacement of the punch. The wrap-around effect is taken into account in the region of the internal radius, using the punch radius as input R_p. It is important to note that the measurement W in equation (11) is the distance between the centers of the radii formed on the shoulders of the punch, instead of the distance between the usually used edges of the channel V, (De Vin, 2000).

$$Z = \frac{\left[W \cdot tan\left(\frac{\beta}{2}\right)\right]}{2} + \left[1 - cos\left(\frac{\beta}{2}\right) - tan\left(\frac{\beta}{2}\right) \cdot sin\left(\frac{\beta}{2}\right)\right] \cdot (R_p + R_m + e) \quad (11)$$

Deriving the equation (11), it is possible to observe that the variable R_p represents the rounding of the sheet at the bottom of the fold, wrap-around, which is also known as the Internal Radius (R_i). Therefore, it is possible to replace the variable R_p with R_i in the equation, forming equation (12).

$$Z = \frac{\left[W \cdot tan\left(\frac{\beta}{2}\right)\right]}{2} + \left[1 - cos\left(\frac{\beta}{2}\right) - tan\left(\frac{\beta}{2}\right) \cdot sin\left(\frac{\beta}{2}\right)\right] \cdot (R_i + R_m + e) \quad (12)$$

3 MATERIALS AND METHODS

The verification of the most accurate analytical method for determining the internal radius and punch displacement on the sheet was done by comparing the analytical results with the results obtained from practical tests. The bends were be performed using the Braffemam® PVH 30100 press brake machine, equipped with CN-120s® control, with a capacity of 100 tons of force and a maximum bending length of three meters. The machine was calibrated with only 14 tons of force, to avoid structural deformations. Rigid tool, with 22 mm channel, was used to ensure no deformation occurs during the mechanical forming process. To perform the tests, the A36 steel material was chosen, as it is widely used in the field of mechanical forming.

To measure the bent angle, a precision goniometer was used, with a minimum division of 0.08° and an expanded uncertainty of 0.206° for a coverage factor of 2. For measuring the sheet thickness, a micrometer with a range of 0 to 25 mm and a minimum division of 0.01 mm was used, with an expanded uncertainty of 0.001 mm for a coverage factor of 2. To measure the punch displacement on the sheet, a dial indicator with a minimum division of 0.01 mm was used, with an expanded uncertainty of 0.001 mm for a coverage factor of 2. The internal radius formed was measured using a profile projector with a minimum division of 0.001 mm, with an expanded uncertainty of 0.005 mm for the X-axis and 0.006 mm for the Y-axis, using a coverage factor of 2. Diascopic projection with a magnification of 10X was used for the measurement.

The equation for sample size was used for an unknown or infinite population, using a confidence level of 95% and a margin of error of 3%, in order to determine the required sample size for measuring thickness, degree, and penetration.

To perform the determination of the internal radius, the equation for the arc width and the arc height was used, as given by the equations (13) and (14). Measurements were taken at different points within the plastic deformation region of the component in order to verify if the internal radius is constant.

$$c = \frac{C_s}{2} \quad (13)$$

$$R_i = \frac{{c_s}^2 \cdot {H_r}^2}{2 \cdot H_r} \quad (14)$$

The displacement results of the punch on the sheet to achieve a certain angle was compared with those obtained from the analytical equations. The final results of the analytical equations was calculated using equation (11) (9), using the values of the internal radius R_i provided by the equations shown in Table 1, either concatenated or not with the estimated values of springback, as presented in section 2.2, using equation (9). The springback factor used will be the one presented in Table 2 and calculated using equation (10). Each of the presented variations will be referred to as a method, making it easier to distinguish. The composition of the methods is presented in Table 4.

Table 3 - Calculation method

	Penetration Z	Internal radius R_i	Springback factor K_r
Method 1	Equation (12)	Equation (1)	1
Method 2	Equation (12)	Equation (2)	1
Method 3	Equation (12)	Equation (3)	1
Method 4	Equation (12)	Equation (4)	1
Method 5	Equation (12)	Equation (5)	1
Method 6	Equation (12)	Equation (6)	1
Method 7	Equation (12)	Equation (7)	1
Method 8	Equation (12)	Equation (8)	1
Method 9	Equation (12)	Equation (1)	Table 2
Method 10	Equation (12)	Equation (2)	Table 2
Method 11	Equation (12)	Equation (3)	Table 2
Method 12	Equation (12)	Equation (4)	Table 2
Method 13	Equation (12)	Equation (5)	Table 2
Method 14	Equation (12)	Equation (6)	Table 2
Method 15	Equation (12)	Equation (7)	Table 2
Method 16	Equation (12)	Equation (8)	Table 2
Method 17	Equation (12)	Equation (1)	Equation (10)
Method 18	Equation (12)	Equation (2)	Equation (10)
Method 19	Equation (12)	Equation (3)	Equation (10)
Method 20	Equation (12)	Equation (4)	Equation (10)
Method 21	Equation (12)	Equation (5)	Equation (10)
Method 22	Equation (12)	Equation (6)	Equation (10)
Method 23	Equation (12)	Equation (7)	Equation (10)
Method 24	Equation (12)	Equation (8)	Equation (10)

For both the calculation of the internal radius and punch displacement, the best method will be the one that demonstrates the highest accuracy when compared to the practical results.

4 RESULTS

Measurements of the punch displacement in the Z-direction, thickness, bend angle, and internal contour were performed to determine the sample size, as shown in Table 4. The calculations of the sample size indicated that for the desired characteristics, a quantity of 10 measurements per piece would be sufficient (excluding the Z penetration, as it can only be measured once). To achieve the desired confidence levels, it was necessary to perform tests on thirteen samples.

Table 4. Thickness, grade and Z-offset measurement results.

	e [mm]	β [°]	Z [mm]
Sample 1	2,01	90,03	9,28
Sample 2	2,00	89,99	9,28
Sample 3	1,98	90,00	9,28
Sample 4	1,99	90,60	9,28
Sample 5	1,99	89,58	9,28
Sample 6	2,01	90,93	9,28
Sample 7	1,98	90,50	9,28
Sample 8	2,01	90,08	9,28
Sample 9	2,00	90,83	9,28
Sample 10	2,01	90,25	9,28
Sample 11	2,00	90,00	9,28
Sample 12	2,01	90,08	9,28
Sample 13	2,01	90,98	9,28

The Table 5 presents the radii that the semicircle should assume in order to maintain equality between the calculation of deflection and cord.

Table 5 - Shape measurement of the inner crease region

Measurement	Axis Y [mm]	Axis X [mm]	R_i [mm]
Point 1	$0{,}150 \pm 0{,}006$	$1{,}468 \pm 0{,}131$	$1{,}870 \pm 0{,}176$
Point 2	$0{,}200 \pm 0{,}006$	$1{,}783 \pm 0{,}085$	$2{,}086 \pm 0{,}096$
Point 3	$0{,}300 \pm 0{,}006$	$2{,}338 \pm 0{,}122$	$2{,}427 \pm 0{,}100$
Point 4	$0{,}400 \pm 0{,}006$	$2{,}764 \pm 0{,}133$	$2{,}587 \pm 0{,}077$
Point 5	$0{,}500 \pm 0{,}006$	$3{,}129 \pm 0{,}091$	$2{,}698 \pm 0{,}054$
Point 6	$0{,}600 \pm 0{,}006$	$3{,}483 \pm 0{,}096$	$2{,}827 \pm 0{,}050$
Point 7	$0{,}700 \pm 0{,}006$	$3{,}803 \pm 0{,}113$	$2{,}933 \pm 0{,}053$
Point 8	$0{,}800 \pm 0{,}006$	$4{,}111 \pm 0{,}094$	$3{,}040 \pm 0{,}040$
Point 9	$0{,}900 \pm 0{,}006$	$4{,}380 \pm 0{,}107$	$3{,}115 \pm 0{,}042$
Point 10	$1{,}000 \pm 0{,}006$	$4{,}658 \pm 0{,}120$	$3{,}212 \pm 0{,}044$
Point 11	$1{,}200 \pm 0{,}006$	$5{,}190 \pm 0{,}113$	$3{,}406 \pm 0{,}036$

It has been observed that the geometry of the internal curvature of the bent sheet metal is not identical to that of a semicircle with a constant radius. Instead, it closely resembles a parabolic shape, (Benson, 2015b). Figure 2 shows the profiles of two bent sheets measured using a profile projector.

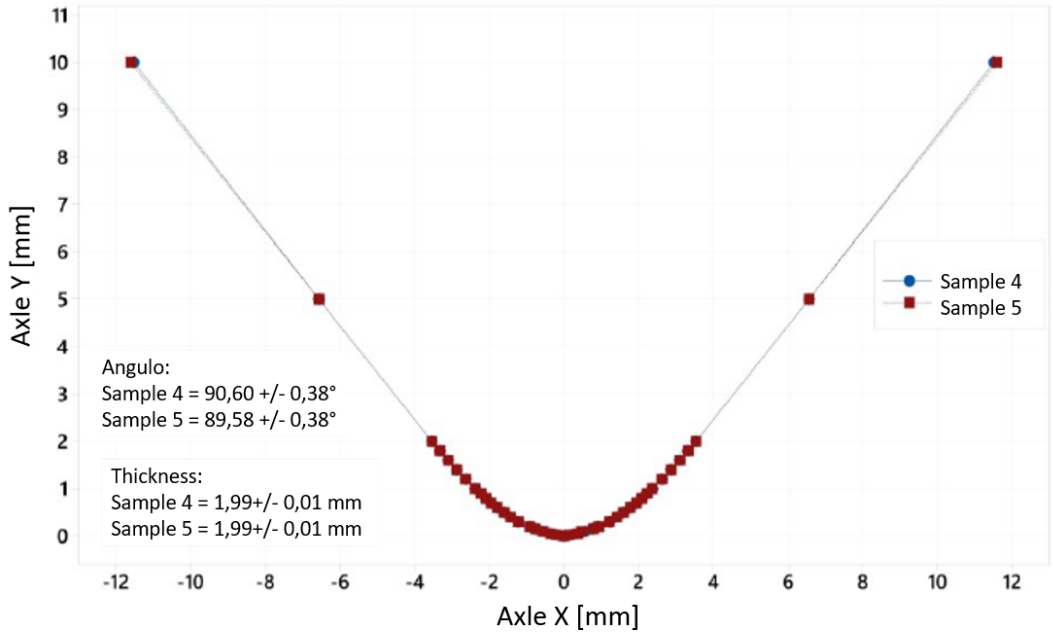

Figure 2. Curvature geometry of the elastic, elastoplastic and plastic region of parts 4 and 5.

Expanding the graph to the region of elastoplastic and plastic deformation of piece four, it can be observed that the geometry closely resembles that of a parabola, as it exhibits a good correlation and low residual values, as shown in Figure 3.

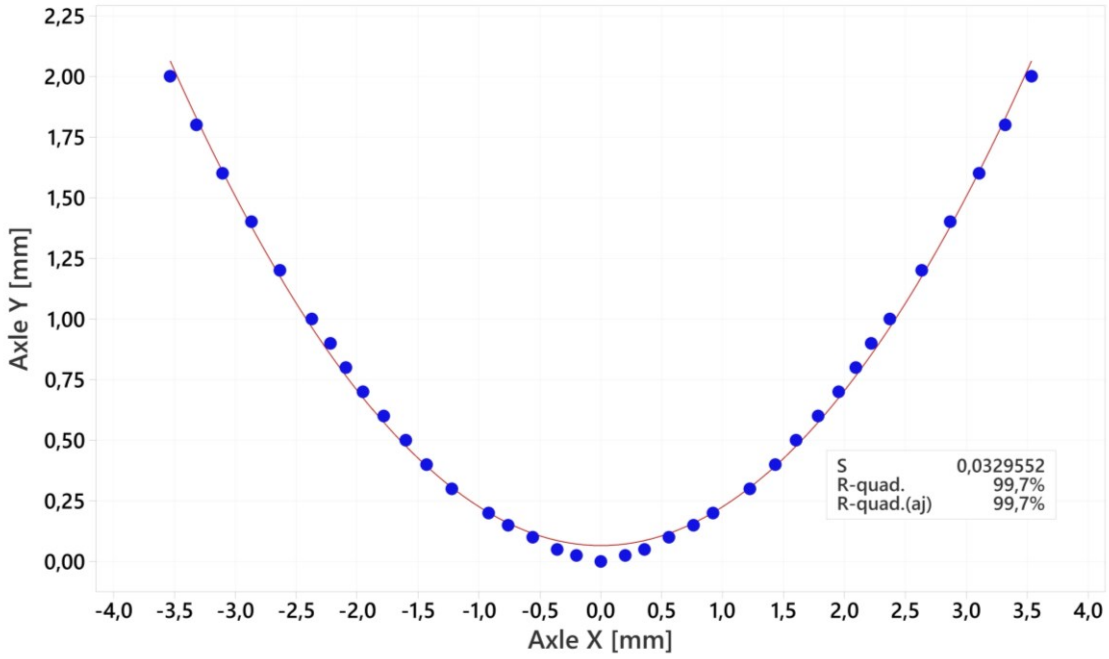

Figure 3. Polynomial regression on part 4.

The Table 6 shows the results of the analytical calculations for the methods presented in Table 3. It can be observed that method 24 achieved the closest approximation to the observed penetration in practical tests, according to Table 4.

Table 6 - Results of analytical equations

	R_i [mm]	K_R	β_{Kr} [°]	Z [mm]
Method 1	3,96	1	90	8,58
Method 2	3,80	1	90	8,65
Method 3	1	1	90	9,81
Method 4	3,71	1	90	8,69
Method 5	0,92	1	90	9,84
Method 6	40,92	1	90	-6,73
Method 7	4,02	1	90	8,56
Method 8	4,02	1	87,72	8,81
Method 9	3,96	0,99	89,09	8,68
Method 10	3,80	0,99	89,09	8,75
Method 11	1	0,99	89,09	9,95
Method 12	3,71	0,99	89,09	8,79
Method 13	0,92	0,99	89,09	9,98
Method 14	40,92	0,99	89,09	-7,05
Method 15	4,02	0,99	89,09	8,66
Method 16	4,02	0,99	89,09	8,91
Method 17	3,96	0,97	87,11	8,90
Method 18	3,80	0,97	87,11	8,97
Method 19	1	0,97	87,11	10,24
Method 20	3,71	0,97	87,11	9,01
Method 21	0,92	0,97	87,11	10,28
Method 22	40,92	0,97	87,11	-7,78
Method 23	4,02	0,97	87,11	8,88
Method 24	4,02	0,97	84,76	9,14

To perform the calculations presented in Table 6, the input data used were taken from Table 7.

Table 7 - Values used in equation (12)

Feature	Abbreviation	Value
Internal angle	β	90°
Thickness	e	2 mm
Die opening	W	23,76 mm
Radius on the shoulders of the die	R_m	2 mm

5 CONCLUSION

Based on the conducted research and market experience in the field of sheet metal bending, it is evident that providing better information to operators and designers of bent parts would increase process speed and reduce losses from parts with dimensions outside tolerance. There are limited studies in this area, and they are typically of a purely academic nature, which makes their practical application difficult or indirect.

When comparing the results obtained through analytical calculations and practical measurements, it was observed that replacing the original value of R_p suggested by De Vin (2000), due to the wrap-around phenomenon, with values closer to reality, calculated by the equations of R_i, improves the accuracy of the punch penetration calculation. It was also observed that among the various equations available for calculating the internal radius, those proposed by Benson achieved the best results, closely matching the experimentally obtained measurements. The springback factor K_r also proved effective in approximating the calculated value to the actual value.

Further tests are needed with different tool presets and sheet thicknesses to confirm that method 24 is the most appropriate for calculating punch penetration. Measuring the internal angle during bending to assess elastic return would assist in formulating the methods, as the present article works with two variables, R_i and K_r. Developing a system that can measure elastic return would provide a more accurate means of determining the formed internal radius during bending and further improve the prediction of punch displacement.

The results of this study guide the steps to be taken in developing tables and charts to assist operators of CN bending machines and designers in the cutting and forming field.

6 REFERENCES

Benson, Steve, 2015a. *How to calculate the air-formed radius of different bend angles (web publications)*. Available at: https://www.thefabricator.com/thefabricator/article/bending/how-to-calculate-the-air-formed-radius-of-different-bend-angles. Accessed on: 11 Dec. 2022.

Benson, Steve, 2015b. *Predicting the inside radius when bending with the press brake (web publications)*. Available at: https://www.thefabricator.com/thefabricator/article/bending/predicting-the-inside-radius-when-bending-with-the-press-brake. Accessed on: 11 Dec. 2022.

De Vin, Leo J., 2000. "Curvature prediction in air bending of metal sheet". *Journal of Materials Processing Technology*, vol. 100, no. 1, p. 257–261.

De Vin, Leo J; Lutters, Eric; Kals, H J J; Vin, Leo J De; Lutters, Eric; Kals, H J J., 1994. *A Process Model for Air Bending in CAPP Applications*. 1994. Shemet [...]. [*S. l.*: *s. n.*], p. 17–28.

Hertzberg, Richard W.; Vinci, Richard Paul; Hertzberg, Jason L., 2012. *Deformation and fracture mechanics of engineering materials*. , p. 755.

IBGE. *PIA-Produto | IBGE*. [*s. d.*]., 2020. Instituto Brasileiro de Geografia e Estatística, Estatisticas, Ecônomicas, Indústia e Construção, Pesquisa Industrial Anual - Produção. Available at: https://www.ibge.gov.br/estatisticas/economicas/industria/9044-pesquisa-industrial-anual-produto.html?=&t=resultados. Accessed on: 7 May 2023.

Lange, Kurt, 1985. *Handbook of metal forming*. [*S. l.*: *s. n.*], Michigan, U.S.A.

Miranda, S.; Pacheco, J.; Santos, Abel D.; Amaral, R., 2014. "The use of finite element analysis on bending radius and springback predition on CNC press brakes programing". *World Congress on Computational Mechanics* [...]. [*S. l.*: *s. n.*].

Ridane, N.; Jaksic, D.; Kleiner, Matthias; Heller, B., 2005. "Enhanced Semi-Analytical Process Simulation of Air Bending". *Advanced Materials Research*, vol. 6–8, p. 729–736.

Schuler, 1998. *Metal Forming Handbook.* [*S. l.*: *s. n.*], Berlin Heidelberg, Germany.

Strano, Matteo; Semeraro, Quirico; Iorio, Lorenzo; Sofia, Roberto, 2018. "Hierarchical Metamodeling of the Air Bending Process". *Journal of Manufacturing Science and Engineering, Transactions of the ASME*, vol. 140, no. 7, 1.

7 RESPONSIBILITY NOTICE

The author is the only responsible for the printed material included in this paper.